

Project No. 09-804

# Development of Subspace-Based Hybrid Monte Carlo-Deterministic Algorithms for Reactor Physics Calculations

---

## Reactor Concepts R&D

Dr. Hany Abdel-Khalik

North Carolina State University

**In collaboration with:**

Los Alamos National Laboratory

Sandia National Laboratory

Rob Versluis, Federal POC

Emily Shemon, Technical POC

**Title: Development of Subspace-Based Hybrid Monte Carlo Deterministic Algorithms for Reactor Physics Calculations**

Authors: Qiong Zhang and Hany S. Abdel-Khalik

Affiliation: North Carolina State University, Raleigh, NC 27695-7909

Corresponding Author: Hany S. Abdel-Khalik

Phone: (919)515.4600

Fax: (919)515.5115

Email: [qzhang7@ncsu.edu](mailto:qzhang7@ncsu.edu), [abdelkhalik@ncsu.edu](mailto:abdelkhalik@ncsu.edu)

Total Number of Pages: 37 (including this page)

Number of Tables: 8

Number of Figures: 9

**Development of Subspace-Based Hybrid Monte Carlo Deterministic Algorithms  
for Reactor Physics Calculations**

Qiong Zhang and Hany S. Abdel-Khalik

**ABSTRACT**

The development of hybrid Monte-Carlo-Deterministic (MC-DT) approaches, taking place over the past few decades, have primarily focused on shielding and detection applications where the analysis requires a small number of responses, i.e., at the detector location(s). This work further develops a recently introduced global variance reduction approach, denoted by the SUBSPACE approach, and extends its application to realistic reactor analysis problems, where responses are required everywhere in the phase space. The SUBSPACE approach is designed to allow the use of MC simulation, currently limited to benchmarking calculations, for routine engineering calculations. By way of demonstration, the SUBSPACE approach is applied to assembly level calculations used to generate the few-group homogenized cross-sections. These models are typically expensive and need to be executed in the order of  $10^3$ - $10^5$  times to properly characterize the few-group cross-sections for downstream core-wide calculations. Applicability to k-eigenvalue core-wide models is also demonstrated in this work. Given the favorable results obtained in this work, we believe the applicability of the MC method for reactor analysis calculations could be realized in the near future.

*Key Words:* Hybrid Monte Carlo-Deterministic, Global Variance Reduction,

FW-CADIS, SUBSPACE Approach

## I. INTRODUCTION

Monte Carlo (MC) methods have been applied in computing the fundamental mode eigen-function of critical systems since the 1950s [1-4]. The use of Monte Carlo simulation in reactor design and analysis calculations has been promoted in recent years to preclude the need for the simplifying assumptions of deterministic methods [5]. To enable the use of MC instead of deterministic models in the standard reactor physics methodology [6], one must rely on global variance reduction (GVR) techniques to accelerate MC convergence. This follows as in the existing reactor physics methodology, the neutronic solver must be executed many times which renders MC simulation an impractical approach for routine calculations. To demonstrate this situation, a short overview of the existing reactor physics methodology is given next.

The reactor core is divided up into smaller regions, often chosen to represent full or parts of a fuel assembly taken at different axial levels. Lattice physics (or assembly) calculations are used to analyze these regions in more detail, often done with many energy groups and fine spatial and angular mesh. The flux solution from lattice physics calculations is used to generate cross-sections that are homogenized over coarser energy groups and spatially over each region in a manner that preserves reaction rates over the various regions. The few-group cross-sections are then used in core-wide simulation where the geometrical, energy, and spatial details of the regions are now smeared which reduces the effective dimensionality of the core-wide problem. Given the reliance of the flux solution from lattice physics calculations on

the isotopic concentration, the fuel temperature, the coolant temperature and/or voiding, presence of poison in the coolant, amount of control rod insertion, etc., the few-group cross-sections must be generated at a matrix of different conditions to enable one to interpolate the correct value for core-wide simulation. This is a formidable task as for typical LWR models the number of these conditions is overwhelmingly large. Take for example a BWR model, one typically has in the order of 30 lattice designs, each depleted using lattice physics calculations to end of life with about 50 depletion steps. This is often repeated with 3 different voiding histories, e.g. no voiding, medium voiding, and high voiding. This is important as the increased voiding affects the spectrum and subsequently the depletion characteristics. At each depletion step, about 5 different branch calculations are executed. In each branch calculation, one parameter, e.g. fuel temperature increase or decrease, control rod insertion, etc., is changed and another flux solution is obtained. The total number of flux solutions for a typical BWR is  $30 \times 50 \times 3 \times 5 = 22500$ . If each flux solution takes in the order of few seconds, which is possible with highly customized commercial codes, these calculations can be completed over a short period of time. With MC models however, unless one has a reasonably fast convergence scheme, the use of MC would be infeasible for routine reactor physics calculations.

To address this challenge, variance reduction techniques have been developed to accelerate MC convergence. The idea is that if one has an approximate idea about the solution, one can use that knowledge to bias MC particles. For adjoint-based variance reduction techniques, which represent our current interest, a simplified

deterministic model is used to calculate an adjoint flux for the response of interest, say a detector response placed somewhere in the reactor core. Given that the adjoint flux can be shown mathematically to describe the importance of particles at different points in the phase space, one can design weight window maps based on the adjoint information to bias MC particles. This is done by splitting particles that are important and playing Russian roulette with particles that are less important. The idea has been successfully demonstrated in the FW-CADIS methodology [6], which generalizes the idea of variance reduction to problems with global responses, i.e., that is when responses are desired everywhere in the phase space. This is done by employing an additional deterministic forward flux solution to assign more weight to regions with low flux and less weight to regions with high flux which renders a uniform variance reduction over all responses of interest. An assembly model represents such an example where the flux is required everywhere in the assembly to properly homogenize the cross-sections.

Over the past couple of years, a new approach, denoted by the SUBSPACE approach [7], was introduced to perform GVR with three primary advantages over existing FW-CADIS methodology. First, the forward flux solution is not required, which results in considerable time savings especially for eigenvalue problem with dominance ratio close to unity. Second, via the use of the so-called pseudo responses, representing random linear combinations of the original responses, the number of MC particles required to reach a given level of variance reduction is significantly reduced. Finally, the approach allows one to split the total number of MC particles over

multiple trains of MC simulation, which improves the efficiency of the methods by allowing one to take advantage of parallel computing environment.

In previous work, the figure of merit (FOM) of the SUBSPACE approach is calculated, which was found to be in the range of 2-10 times faster than the FW-CADIS approach [7]. The lower range for the gain is for source-driven problems with small dimensionality in terms of the responses and the complexity of the geometry and energy details. The gain increases as the dimensionality of the model increases and reaches its maximum for eigenvalue core-wide problems.

## II. SUBSPACE APPROACH-BASED IMPLEMENTATION

In its standard form, the k-eigenvalue transport equation is written as:

$$[\Omega \cdot \nabla + \sum_T(\bar{r}, E)]\psi(\bar{r}, E, \Omega) = \iint \psi(\bar{r}, E', \Omega') \sum_S(\bar{r}, E' \rightarrow E, \Omega \cdot \Omega') d\Omega' dE' + \frac{1}{k_{eff}} \frac{\chi(E)}{4\pi} \iint \nu \sum_F(\bar{r}, E') \psi(\bar{r}, E', \Omega') d\Omega' dE' \quad (1)$$

where the standard notations are used. The k-eigenvalue problem can conveniently be written in operator notation as:

$$L\bar{\psi} = \frac{1}{k_{eff}} F\bar{\psi}, \quad (2)$$

The problem above is amenable to solution by Deterministic, analog Monte-Carlo and hybrid Deterministic Monte-Carlo methods. Typically the user is interested in a set of responses given by the inner product of the forward flux solution  $\bar{\psi}$  and a response function  $\bar{\sigma}$  of the form:

$$u = \langle \bar{\psi}, \bar{\sigma} \rangle \quad (3)$$



If only one response is sought, it is straight-forward to tailor an adjoint function to this response. The adjoint function assigns importance values to different points in phase space based on their contribution to the response of interest:

$$L^* \bar{\psi}_i^* = \frac{\partial u_i}{\partial \bar{\psi}} = \bar{\sigma}_i, \quad (4)$$

where  $L^*$  is the adjoint transport operator and  $\bar{\psi}^*$  is the importance map associated with response. When applying the weight-window, a permissible range of weights can then be assigned to various regions in phase space based on this adjoint function: If the particle weight is below the specified range, it is Russian-rouletted and if it is above the range, it is split into multiple particles. In GVR problems, responses are desired everywhere, i.e.

$$u_i = \langle \bar{\psi}, \bar{\sigma}_i \rangle, \text{ and } i = 1, \dots, I, \quad (5)$$

where  $I$  is the total number of responses, often representing the flux or reaction rates calculated at many regions in the phase space.

To ensure a uniform reduction of variances over the phase space, one needs to develop an adjoint function that helps bias MC particles towards all responses of interest [8]. In FW-CADIS, the adjoint source is formulated as a weighted sum of the individual responses' adjoint sources, weighted by the inverse of the forward flux [9], i.e. the following forward and adjoint problems are solved:

$$\begin{aligned} L\bar{\psi} &= \frac{1}{k} F\bar{\psi} \Rightarrow u_i = \langle \bar{\psi}, \bar{\sigma}_i \rangle \\ L^* \bar{\psi}^* &= \sum_{i=1}^I \frac{1}{u_i} \frac{\partial u_i}{\partial \bar{\psi}} = \sum_{i=1}^I \frac{\bar{\sigma}_i}{u_i}, \end{aligned} \quad (6)$$

This approach is based on a sound engineering intuition in which more particles are sent to regions in the phase space where the flux is expected to be low and less particles to high flux regions. This helps render uniform variance reduction over all responses of interest.

In contrast, the SUBSPACE approach is based on a mathematical approach that takes advantage of the correlation between the various responses [7]. This helps reduce the effective number of responses for which weight-windows are to be tailored. This is achieved by generating adjoint functions for the so-called pseudo-responses which are random linear combinations of the original responses:

$$\tilde{u}_j = \sum_{i=1}^I \bar{\eta}_{i,j} u_i \quad (7)$$

(where  $\bar{\eta}_j \in \mathbf{R}^I$  is a randomly generated vector). Although, they lack physical meaning, these pseudo responses allow one identify the minimum number of effective responses and their associated weight windows required to achieve the same level of variance reduction that would be achieved if all single-response weight window maps are employed to reduce variances for all responses one at a time (see Ref. [7] for details). The key reason for their success lies in the use of random numbers, which have been shown by nuclear researchers [21] and independently by mathematicians to help identify correlations/patterns in large data sets. Using the definition for  $u_i$  from Eq. (4), one can write:

$$\begin{aligned}\tilde{u}_j &= \sum_{i=1}^I \eta_{i,j} \langle \bar{\psi}, \bar{\sigma}_i \rangle = \left\langle \bar{\psi}, \sum_{i=1}^I \eta_{i,j} \bar{\sigma}_i \right\rangle \\ L^* \tilde{\psi}_j^* &= \frac{\partial \tilde{u}_j}{\partial \bar{\psi}} = \sum_{i=1}^I \eta_{i,j} \bar{\sigma}_i\end{aligned}\quad (8)$$

In our context, the responses of interest are the few-group homogenized cross-sections given by the general form:

$$\Sigma_{x,g} = \frac{\langle \phi_g, \sigma_{x,g} \rangle}{\phi_g}, \quad (9)$$

where  $x$  denotes the reaction type ( $x$ =fission, capture, scattering).

The pseudo response would correspondingly be described as:

$$\tilde{u}_x = \sum_g \sum_x w_{x,g} \langle \phi_g, \sigma_{x,g} \rangle \quad (11)$$

where  $x$  now stands for  $x$ =fission, capture, scattering and flux and  $w_{x,g}$  represents the weighting factor.

The adjoint source is constructed as:

$$L^* \tilde{\phi}_x^* = \frac{\partial \tilde{u}_x}{\partial \phi} = \sum_g \sum_x w_{x,g} \sigma_{x,g} \quad (12)$$

Therefore, given the desired problem-specific cross section as the response of interest, the pseudo response is constructed as a linear combination of weighted original cross section responses from given libraries. For the SUBSPACE approach, the weighting factors are sampled from a statistical distribution and an algorithm is introduced to obtain the optimized number of correlations between given responses.

For the FW-CADIS approach, the weighting factors are obtained from a forward calculation and calculated as the inverse of the response, in this case: the reaction rate.

The algorithm to implement the SUBSPACE approach is described as follows:

Requirements:

- A general methodology that employs an importance map  $\bar{\psi}_i^*$  to bias Monte Carlo particles towards a given response  $u_i$ .
- The capability to calculate an importance map  $\tilde{\psi}_j^*$  for a pseudo response defined as a random linear combination of the original  $I$  responses as defined in Eq. (11).

Objective:

- Identify  $r$  pseudo response, and employ them to reduce variance for all  $I$  responses.

Algorithm:

- a) Estimate the rank  $r$ . If no prior knowledge about the rank is available, pick a small value, e.g.  $5 < r < 20$ , and execute step b. Calculate the SVD of the matrix containing the importance maps for the  $r$  pseudo responses:  $[\tilde{\psi}_1 \quad \tilde{\psi}_2 \quad \dots \quad \tilde{\psi}_r]$ . If the singular values do not significantly decline, increase the estimate for  $r$ .
- b) PARALLEL DO  $j=1, \dots, r$ 
  1. Generate a random vector  $\bar{\eta}_j \in \square^I$
  2. Form a pseudo response  $\tilde{u}_j = \sum_{i=1}^I \eta_{i,j} u_i$
  3. Calculate the importance map  $\bar{\psi}_i^*$  associated with  $\tilde{u}_j$

4. Bias Monte Carlo particles based on the  $\bar{\psi}_i^*$
5. Tally the original  $I$  responses until number of histories is exhausted
6. Record the responses  $u_{i,j}^\mu$  and their standard deviations  $u_{i,j}^\sigma$

END DO

c) COMBINE the responses and their standard deviations from the  $r$  runs as follows:

$$u_i^\mu = u_i^\sigma \sum_{j=1}^r \frac{u_{i,j}^\mu}{(u_{i,j}^\sigma)^2} \quad \text{and} \quad \frac{1}{u_i^\sigma} = \sum_{j=1}^r \frac{1}{(u_{i,j}^\sigma)^2}$$

End Result:

- The  $u_i^\mu$  and  $u_i^\sigma$  are the mean and standard deviation for the  $i^{\text{th}}$  response calculated by the SUBSPACE method.

This algorithm is composed of three steps. Step (a) requires an estimate of the rank  $r$ . Step (b) represents an execution of an existing variance reduction method with a special choice for the pseudo response. Since the importance function is often calculated using an adjoint model, this should be fairly easy to implement for most codes via simple manipulation of the right hand side of the adjoint equation. Next section provides more details on this step for incorporating the SUBSPACE method into the FW-CADIS framework. Step (c) combines the results from the  $r$  executions, each with  $N$  independent histories, under the assumption that they are statistically independent [7].

The adjoint flux map utilized for the SUBSPACE approach is generated using the three-dimensional discrete ordinates code DENOVO [8]. Similar to the FW-CADIS approach, the optimization objective of the SUBSPACE approach is the

group-wise fluxes in fissionable regions [9]. In contrast to the FW-CADIS eigenvalue implementation which requires the solution of a forward eigenvalue problem [10], the SUBSPACE approach solves a single adjoint fixed source problem with the adjoint source being determined as derivatives of the pseudo responses with respect to the adjoint function [7]. From the adjoint function the upper and lower weight window bounds are computed and subsequently the weight window map is written in a format suitable for MCNP [10]. The Monte-Carlo computations are all performed using MCNP.

### **III. EIGENVALUE PROBLEM STUDY**

A three-dimensional quarter core PWR model is employed to compare the performance of the FW-CADIS and the SUBSPACE approaches. The PWR quarter core model features a generic three-dimensional layout. The x-y-z dimensions are 204.25x204.25x335.28cm. The model consists of 48¼ 17x17 fuel assemblies, with 264 fuel rods per assembly each of which features a 3wt% U235/U uniform fuel enrichment. The adjoint fixed-source DENOVO calculations use an S4 level symmetric quadrature and a  $461 \times 461 \times 10$  spatial grid resolving the unit-cells. The 27 neutron and 19 photon energy group libraries included in the SCALE package are employed for generating the adjoint flux maps. For the flux and reaction rate responses, the first 14 neutron groups ( $10.678\text{eV} < E < 20\text{MeV}$ ) define the fast group and the last 13 groups ( $E < 3.059\text{eV}$ ) are thermal. A cross sectional view of the model

is presented in Fig. 1, where green represents moderator and reflector (water) and red the fuel pins.

Continuous-energy MCNP5 simulations are conducted using 50,000 histories/cycle, 2500 active cycles with 500 inactive cycles starting from an initially uniform fission source. FW-CADIS and the SUBSPACE approaches are applied respectively and a thermal flux energy bin from 0.15 to 0.275eV (to be consistent with the response selected by the FW-CADIS work, see Ref [9]) is selected to compare the performance of two approaches. The obtained results of the relative uncertainty associated with the thermal flux are illustrated along the z-dimension for the middle layer (-16.674cm) in the model as shown in Fig. 2. The color bar identifies the percentage of relative uncertainty.

The distribution of relative uncertainties associated with the thermal flux mesh tally (three-dimensional Cartesian array of tallies) in the given energy bin is plotted in Fig. 3 at the mid axial section of the core. Only the cells within the reactor core (i.e. excluding the reflector) are taken into account. The distribution of uncertainties obtained with the FW-CADIS and SUBSPACE approaches are similar demonstrating that for the same number of histories both methods obtain results featuring about the same level of confidence. The standard deviation and the mean value of the distribution of variances obtained with FW-CADIS and SUBSPACE approaches are presented in Table 1. For reference, the analog results are also provided. When applying the SUBSPACE approach, the obtained mean value of variance is 0.0181; while the mean value of variance obtained by performing FW-CADIS approach is

0.0346. Furthermore, the SUBSPACE approach generates a standard deviation of the variance distribution that is 33% lower compared to the same quantity generated by FW-CADIS, which implies a more uniform distribution of variances, which is a desirable feature of variance reduction techniques.

In order to compare the efficiency, the global FOMs of the two approaches are calculated and presented in Table 2. It is important to note that the execution time of DENOVO when applying the SUBSPACE approach is 1/30 compared to the execution time required by FW-CADIS. The primary reason for this is that the FW-CADIS approach requires a forward eigenvalue flux solution [9] while the SUBSPACE approach only requires a source-driven solution. In most realistic core-wide problems, the eigenvalue solution is very expensive because the dominance ratio is very close to 1.0. As a secondary reason, the parallelization associated with the SUBSPACE approach improves the computational efficiency by distributing the work load evenly on multiple processors.

The global FOM is calculated as the inverse product of the mean value of variance distribution and total execution time, which, in this case study, is the sum of the DENOVO execution time and the MCNP execution time. The global FOM is defined as:

$$FOM = \frac{1}{v(t_{DENOVO} + t_{MCNP})}$$

For the analog MC simulation, the total time equals to the MCNP execution time. As shown in Table 2, the global FOM obtained from applying the SUBSPACE



approach is 0.0649 while the global FOM of the FW-CADIS approach is 0.0071. Meanwhile, the analog MC simulation has a global FOM value of 0.000698. These results demonstrate that the SUBSPACE approach shows a 9 times speedup over FW-CADIS, which has been reported previously to show 6-10 speed up over analog MC. Finally, the SUBSPACE approach shows a speed-up of 93 over the analog.

#### **IV. CROSS SECTION FUNCTIONALIZATION STUDY**

A peach-bottom 7\*7 BWR assembly model is employed and rebuilt in this section [7]. The assembly model represents the southeast assembly of a typical 2x2 BWR control cell which contains four assemblies and a cruciform control blade that is not modeled within the scope of this work. The specifications of the BWR assembly are listed in Table 3. The assembly contains 49 fuel rods in a regular 7x7 fuel rod array. Each fuel pin is assigned with a unique fuel composition. The moderator around the fuel pin is separated into unit cells. The 49 unit cells are tallied and homogenized independently as shown in the Fig. 4.

The BWR model is implemented in the MCNP and NEWT computer codes. Both codes compute an identical Keff demonstrating consistency of the two models. NEWT is a multigroup, discrete-ordinates radiation transport code that could be used to prepare collapsed weighted cross sections and perform fixed-source and eigenvalue calculations [11]. NEWT allows plenty flexibility in defining boundary conditions [11]. The 44-group SCALE library is employed and collapsed into thermal group and fast group. The thermal group ranges from 0 through 0.625eV and the fast group

comprises the energy range above 0.625eV [8]. Collapsed cross sections for each energy group are obtained from the 44-group library. An importance map is created based on a NEWT adjoint fixed-source calculation where the sources are constructed from the numerical values of the collapsed 44-group cross section library. The importance map is consequently used in the MCNP calculation and for each material in the assembly the desired responses: functionalized cross sections are obtained.

The material representing unit cell 1 in the assembly serves as an example to compare the performance of different hybrid methods. The analog Monte Carlo simulation completes 2000 active cycles, 20000 histories per cycle in 351.02 minutes. When applying the SUBSPACE approach, the same number of histories is completed in 131.14 minutes and applying FW-CADIS it is completed in 99.72 minutes.

Three different cross section quantities are employed as examples to compare the performance: fission, capture and scattering. The relative uncertainties of the obtained numerical results are shown in Table 4 for thermal and fast energy groups. The SUBSPACE approach obtains an average uncertainty level that is 2~3 times lower compared to the analog for the fast group and 4~5 times lower for the thermal group. Meanwhile, the SUBSPACE approach also shows a much better performance in reducing uncertainty compared to the FW-CADIS approach particularly for the thermal group, where a 50% decrease in term of relative uncertainty is obtained. This is due to the fact that the mean free path for the neutron in a thermal reactor is short which correlates each pin's responses to its nearest neighboring pins. Fast neutrons however have longer mean free path and they are able to visit the entire assembly

from their birth to their death, hence the assembly features are more smeared for fast neutrons than they are for thermal neutrons. Since the thermal responses have more significant meaning compared to the fast flux in reactor physics, therefore, the SUBSPACE approach is particularly meaningful in realistic reactor analysis problems.

The results of the global FOM are shown in Table 5. The global FOM is calculated as:

$$FOM_{GVR} = \frac{1}{v(t_{NEWT} + t_{MCNP})}$$

$$FOM_{analog} = \frac{1}{vt_{MCNP}}$$

It is shown that for the thermal group, the SUBSPACE approach obtains a speedup between 32~38 over the analog and for the fast group a speedup between 9~16 over the analog. On the other hand, FW-CADIS approach obtains a speedup over the analog that is between 19~22 for the thermal group and a speed up between 6~11 for the fast group. Fig. 5 and Fig. 6 plot the GVR methods' speedup for fast and thermal group for fission, capture and scattering independently. The blue bar and the red bar respectively identify the speedup over the analog of the SUBSPACE approach and the FW-CADIS approach. For all the three quantities plotted in both plots, the blue bar shows a more significant increase than the red bar, which shows that the SUBSPACE approach is more efficient than the FW-CADIS approach in accelerating the analog MC procedure for both fast and thermal responses.

## V. DEPLETION STUDY

The 7x7 BWR assembly model described in Section IV is employed in this section for demonstrating the feasibility of the SUBSPACE approach in depletion calculation. The depletion calculation is conducted by TRITON [8]. The 44 group energy library from SCALE, as introduced in Section IV, is employed and collapsed into thermal 0~0.625eV and fast 0.625ev~20MeV groups. The 49 fuel pins are divided into 8 groups based on the different composition for depletion purpose as shown in Fig. 7. The assembly model is simulated under hot condition with a pellet temperature of 900K and a moderator temperature fixed at 600K. A constant power level of 45.220MW/MTU is maintained during the depletion which is split over 5 depletion cycles, each spanning a 100 day period. Throughout the depletion cycles, the computed multiplication factor decreases from 1.08682 to 0.92166. The Burnup level increases from 1.13 GWd/MTU to 19.2 GWd/MTU.

The Monte Carlo calculations are performed using MCNP5. The SUBSPACE approach is implemented for representing GVR methodology. Since the assembly level homogenized cross sections are chosen as the response of interest, the pseudo responses are constructed as a linear combination of weighted original cross section responses from the SCALE library. The analog Monte Carlo is performed independently for comparison. For all depletion cycles, 20000 histories/cycle and 2000 active cycles are completed in the MCNP simulation. As demonstrated in [12], a single weight window in Monte Carlo simulation proves as accurate as multiple specified weight windows for all the depletion cycles. Therefore to guarantee the

maximum efficiency, in this work a single averaged weight window is constructed for all the depletion cycles employing the SUBSPACE approach. The number densities of nuclides are obtained for each depletion cycle from the TRITON calculation and different depletion scenarios are built.

For each depletion scenario, an adjoint fixed-source problem, with the SUBSPACE pseudo response constructed by linearly combining original cross section data from the SCALE library, is solved and the corresponding importance map is obtained. Multiple importance maps (3~5 per depletion cycle) are generated employing the SUBSPACE approach to represent the complete depletion process. All the importance maps are then linearly combined into one single importance map, based on which an “average” weight window is constructed for subsequent Monte Carlo simulations. To compare the performance of the SUBSPACE approach versus analog Monte Carlo, the figure of merits for group fluxes and reaction rates (fission, capture, scattering) at each depletion level are calculated as:

$$FOM_{SUBSPACE} = \frac{1}{v(t_{NEWT} + t_{MCNP})}$$

$$FOM_{analog} = \frac{1}{vt_{MCNP}}$$

For the SUBSPACE approach, the total time is computed as the sum of the deterministic calculation time from the adjoint fixed-source run by NEWT and the Monte Carlo calculation time from the MCNP simulation. For the analog, the total time is the Monte Carlo calculation time by MCNP. The final execution times of SUBSPACE and analog are listed in Table 6. The average time for all depletion runs

is 451.84 minutes for the analog calculation and 149.14 minutes while applying the SUBSPACE approach.

In this study, flux and fission are employed as the two most important quantities to demonstrate the performance of the SUBSPACE approach. The corresponding FOM results are presented in Table 7 and Table 8. The speedups obtained by applying the SUBSPACE approach are plotted in Fig. 8 and Fig. 9 to show how the FOM speedups evolve throughout all the depletion cycles. For both flux and fission throughout all depletion cycles, the FOMs obtained by the SUBSPACE approach gain speedups that are between 40~50 for the thermal group and between 10~20 for the fast group when compared to the analog FOMs. Therefore, the SUBSPACE approach shows a more prominent performance regarding thermal responses as stated in Section 3 that the SUBSPACE approach is particularly efficient in accelerating thermal response calculations. In Fig. 8 and Fig. 9, it is shown that the speedups distribute evenly through the complete depletion process instead of showing an explicit increasing or decreasing trend. This well demonstrates the consistency of the performance of the single average weight window for all the depletion scenarios which is desirable.

## **VI. CONCLUSION**

This work focuses on devising a procedure that enables the use of MC simulation to generate all few-group cross-sections required for core-wide calculations. In particular, we investigate on the generation of the few-group cross-sections, and the impact of depletion on the biasing procedure. Results indicate that

the SUBSPACE approach obtains 8-10 times speedup for fast group and 40-50 times speedup for thermal group over the analog, and the average weight window optimized to address all depletion cycles results in a consistent and effective speedup. In future work, we propose to extend this idea to investigate the impact of other core conditions on the weight windows, such as fuel temperature, coolant temperature and voiding, control rod insertion. If all these changes result in insignificant loss of the speedup, the SUBSPACE approach will be extended to account for all core condition variations.

Furthermore, we will investigate on the use of the GPT-free methodology to reduce the computational cost required to generate all the depletion and branch cases. Based on recent results of applying GPT-free to a realistic assembly models, we expect another two orders of magnitude speed up, since the GPT-free methodology allows one to directly calculate the change in the few-group cross-sections due to changes in core parameters without having to re-execute the MC model.

## **ACKNOWLEDGEMENT**

This work has been supported by a Department of Energy Nuclear Energy University Program grant entitled ‘Development of Subspace-Based Hybrid Monte Carlo-Deterministic Algorithms for Reactor Physics Calculations’.

## **REFERENCES**

1. E.L. KAPLAN, "Monte Carlo Methods for Equilibrium Solutions in Neutron Multiplication", UCRL-5275-T, Livermore National Laboratory (1958).
2. W. GOAD and R. JOHNSTON, "A Monte Carlo Method for Criticality Problems", Nucl. Sci. Eng.5, 371-375 (1959).
3. J. LIEBEROTH, "A Monte Carlo Technique to Solve the Static Eigenvalue Problem of the Boltzmann Transport Equation," Nukleonik 11,213 (1968).
4. M. R. MENDELSON, "Monte Carlo Criticality Calculations for Thermal Reactors," Nucl. Sci Eng. 32, 319-331 (1968).
5. K. SMITH, "Assembly Homogenization Techniques for Light Water Reactor Analysis," Progress in Nuclear Energy, 17, 3 (1986).
6. J.C. WAGNER and S.W. MOSHER, Forward-Weighted CADIS Method for Variance Reduction of Monte Carlo Reactor Analysis, ORNL, Trans. Am. Nucl. Soc. 103, 342-344 (2010).
7. Z. WU, Q. ZHANG and H.S. ABDEL-KHALIK, "On Hybrid Monte Carlo-Deterministic Methods for Reactor Analysis", Nuclear Technology, In print, Dec. 2012.
8. SCALE: A Modular Code System for Performing Standardized Computer Analyses for Licensing Evaluations, ORNL/TM-2005/39, Version 6, Vols. I-III, January 2009.
9. J. C. WAGNER, S. W. MOSHER, "Forward Weighted CADIS Method for Variance Reduction of Monte Carlo Reactor Analysis," Trans. Am. Nucl. Soc. 103. 342-344 (2010).



10. MCNP: A General Monte Carlo N-Particle Transport Code, Version 5, Volume 2: User's Guide.
11. M.D. DEHART, "NEWT: A new transport algorithm for two-dimensional discrete ordinates analysis in non-orthogonal geometries", ORNL/TM-2005/39, UT-Battelle, LLC, Oak Ridge National Laboratory, January (2009).
12. Q. Zhang and H. Abdel-Khalik, "Global Variance Reduction for Monte Carlo Reactor Physics Calculations", Accepted to ANS Winter Meeting, Nov. 11-15, (2012).
13. J.F. BRIESMEISTER, Editor, "MCNP – A General Monte Carlo N-Particle Transport Code, Version 4A," LA-12625, Los Alamos National Laboratory (1993).
14. F.B. BROWN, A Review of Monte Carlo Criticality Calculations-Convergence, Bias, Statistics, Monte Carlo Codes, X-3-MCC, LANL, M&C, May 3-7, Saratoga (2009).
15. Q. ZHANG and H. S. ABDEL-KHALIK, "Adjoint-Based Global Variance Reduction Approach for Reactor Analysis Problems," Proc. Int. Conf. Math. Comp., Rio De Janeiro (2011).
16. J. C. WAGNER, E. D. BLAKEMAN, and D. E. PEPLOW, "Forward-Weighted CADIS Method for Variance Reduction of Monte Carlo Calculations of Distributions and Multiple Localized Quantities," Proc. Int. Conf. Math. Comp. Saratoga Springs, NY (2009).

17. A. HAGHIGHAT, J. C. WAGNER, "Monte Carlo Variance Reduction with Deterministic Importance Functions," Progress in Nuclear Energy, Vol 42, No. 1 (2003).
18. J. C. WAGNER, E. D. BLAKEMAN, D.E. PELOW, "Forward-Weighted CADIS Method for Global Variance Reduction," ANS Annual Meeting, November 11-15, Washington, DC (2007).
19. J. C. WAGNER, D. E. PELOW, S. W. MOSHER, T. M. EVANS, "Review of Hybrid (Deterministic/Monte Carlo) Radiation Transport Methods, Codes, and Applications at Oak Ridge National Laboratory," Joint International Conference on Supercomputing in Nuclear Applications and Monte Carlo 2010, Hitotsubashi Memorial Hall, Tokyo, Japan (2010).
20. Q. ZHANG and H. S. ABDEL-KHALIK, "Hybrid Monte Carlo-Deterministic Approach Global Variance Reduction," Transactions of the American Nuclear Society, Hollywood Florida (2011).
21. H.S. ABDEL-KHALIK, "Adaptive Core Simulation," Ph.D. Dissertation (2007).

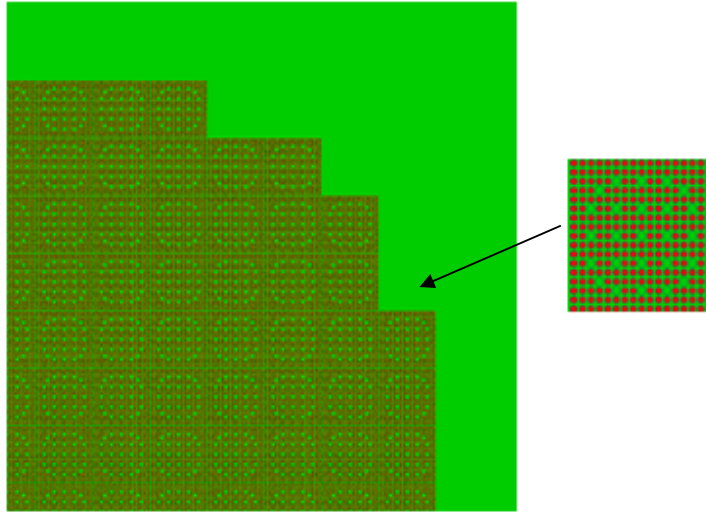


Fig.1. A Section View of 3-D PWR Quarter Core Model

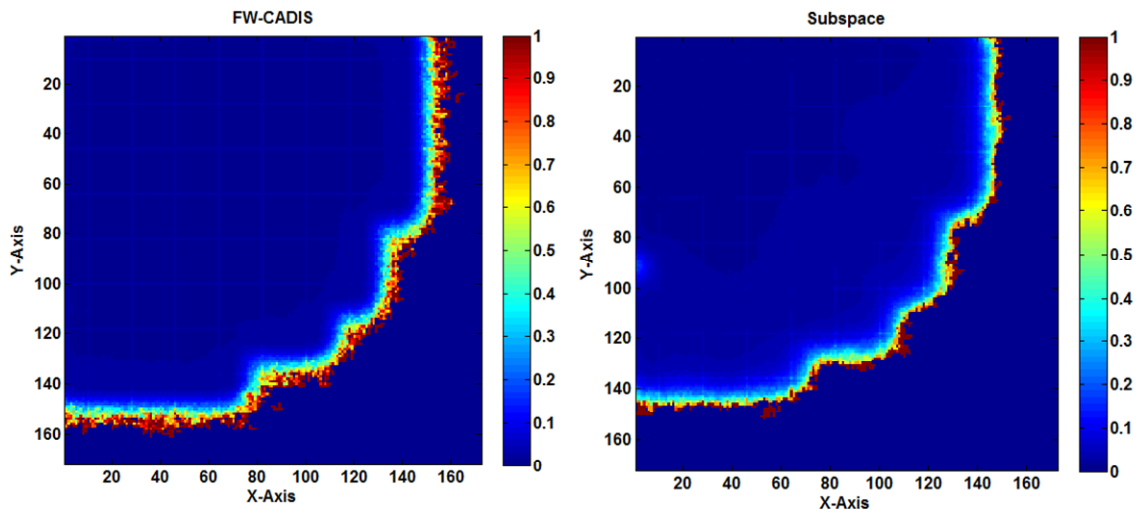


Fig. 2. Relative Uncertainties Computed Using MCNP 5 with FW-CADIS and SUBSPACE Approaches for Tallied Thermal Flux. Colorbar identifies the percentage of relative uncertainty.

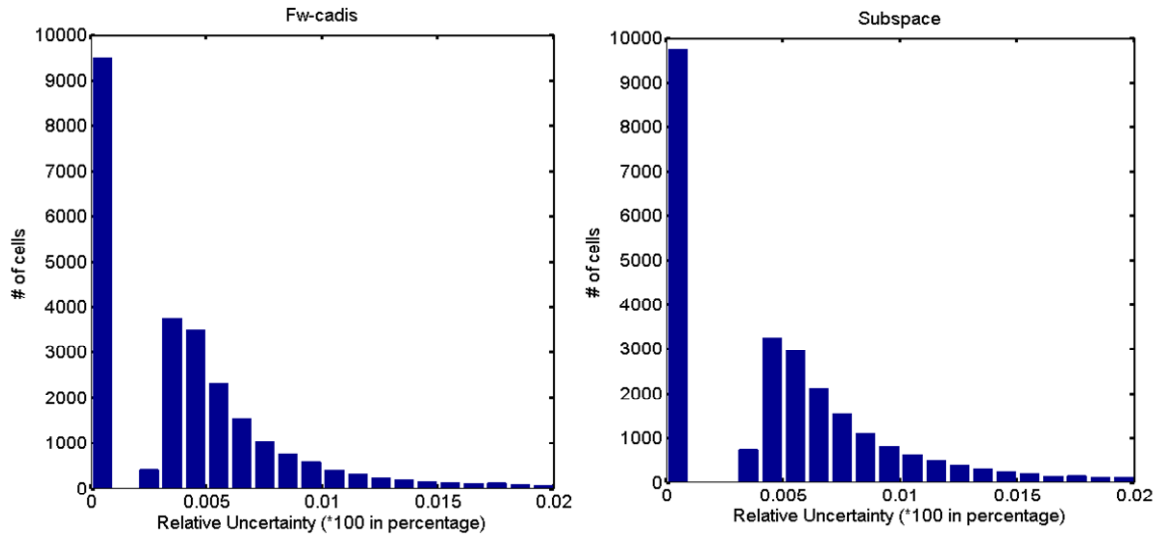


Fig. 3. Relative Uncertainty Distribution for Tallied Thermal Flux using FW-CADIS and SUBSPACE Approaches

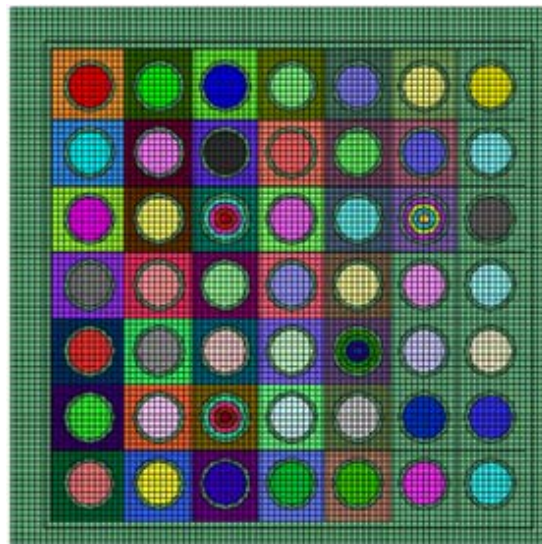


Fig.4. BWR Assembly Model

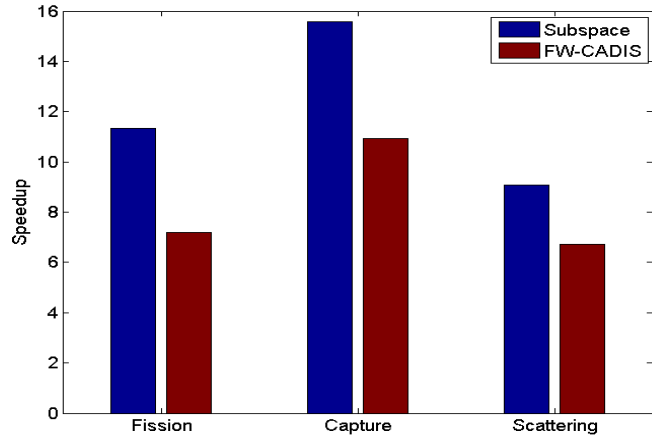


Fig.5. GVR Calculation Speedup for Fast Group

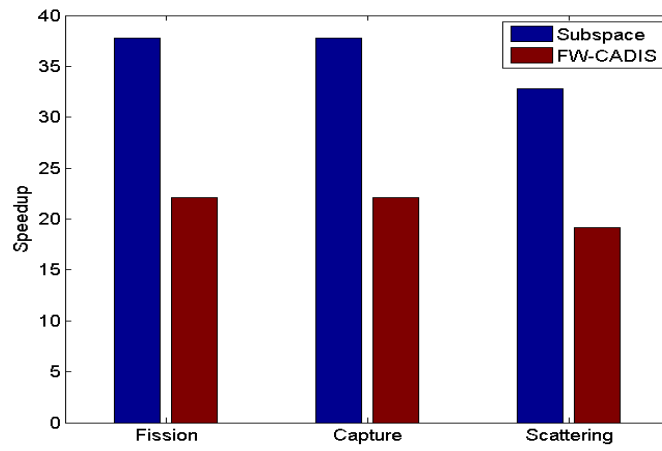


Fig.6. GVR Calculation Speedup for Thermal Group

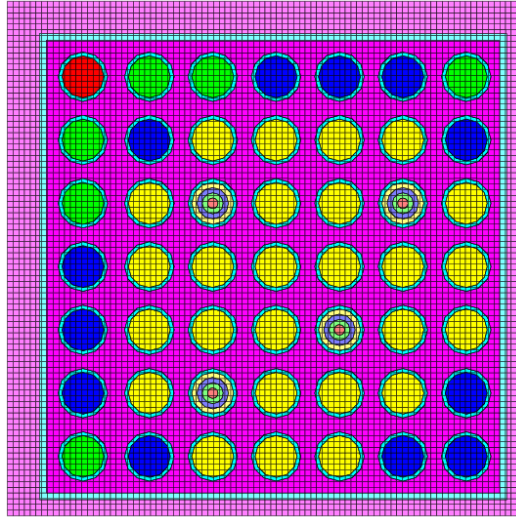


Fig.7. Depletion Pattern of BWR Assembly Model

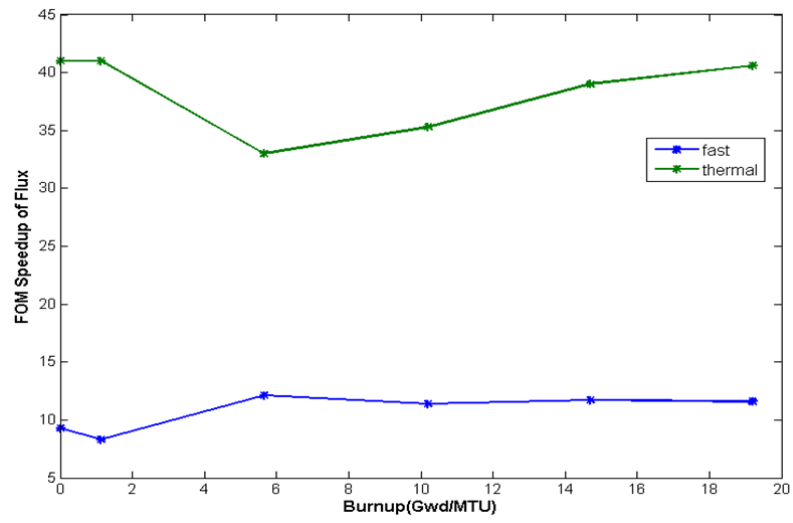


Fig.8. FOM Speedup of Flux through Depletion

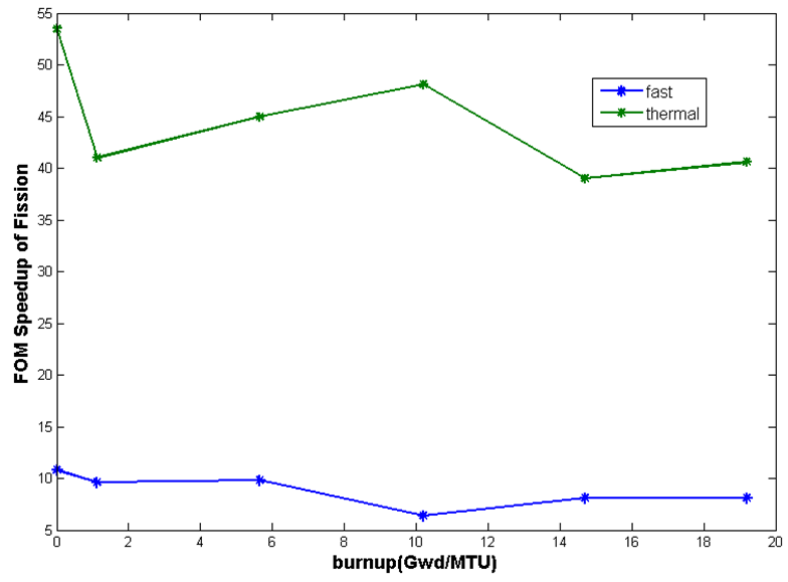


Fig.9. FOM Speedup of Fission through Depletion



Table 1: Standard Deviation and Mean Value of the Variance Distribution

	Stdev of variance	Mean of variance
FW-CADIS	0.1503	0.0346
SUBSPACE	0.1017	0.0181
Analog	0.2145	0.0588

Table 2: Execution Time and Global FOM

	Execution Time (mins)			FOM
	Denovo	MCNP	Total	
SUBSPACE	90.83	761.76	852.59	0.0649
FW-CADIS	2883.05	1208.91	4091.96	0.0071
Analog	N/A	24364.05	24364.05	0.000698

Table 3: BWR Model Specification

Assembly Pitch (cm)	15.24
Fuel Pitch (cm)	1.8745
Fuel Rod Diameter (cm)	1.2116
Cladding Thickness(cm)	0.1092
Canning Thickness (cm)	0.2032
Material Temperature (K)	552.833

Table 4: Relative Uncertainty of Homogenized Cross Sections

	Fast Group (%)			Thermal Group (%)		
	Analog	SUBSPACE	FW-CADIS	Analog	SUBSPACE	FW-CADIS
Fission	0.103	0.050	0.072	0.106	0.028	0.042
Capture	0.206	0.085	0.117	0.106	0.028	0.042
Scattering	0.078	0.042	0.057	0.099	0.028	0.042

Table 5: Global FOM of Homogenized Cross Sections

	Fast Group					
	Analog	SUBSPACE	Speed-up	Analog	FW-CADIS	Speed-up
Fission	2.68E+03	3.05E+04	11.35	2.68E+03	1.92E+04	7.18
Capture	6.70E+02	1.04E+04	15.58	6.70E+02	7.31E+03	10.92
Scattering	4.67E+03	4.23E+04	9.07	4.67E+03	3.13E+04	6.71
	Thermal Group					
	Analog	SUBSPACE	Speed-up	Analog	FW-CADIS	Speed-up
Fission	2.52E+03	9.53E+04	37.81	2.52E+03	5.57E+04	22.10
Capture	2.52E+03	9.53E+04	37.81	2.52E+03	5.57E+04	22.10
Scattering	2.90E+03	9.53E+04	32.79	2.90E+03	5.57E+04	19.16

Table 6: Total Execution Time of Depletion Calculations

Depletion Cycle	Total Execution Time (mins)	
	Analog	SUBSPACE
1	402.6	120.3
2	421.6	135.2
3	441.8	146.1
4	472.1	165.2
5	521.1	178.9

Table 7: The FOM Comparison of Flux

Depletion Cycle	FOM				SUBSPACE Speedup	
	Analog		SUBSPACE		Fast	Thermal
	Fast	Thermal	Fast	Thermal		
No depletion	9934.2	5068.5	92304.0	207684.0	9.3	41.0
1	9934.2	5068.5	82161.1	207684.0	8.3	41.0
2	6287.0	6287.0	76059.9	207684.0	12.1	33.0
3	5883.0	5883.0	67257.2	207684.0	11.4	35.3
4	5329.8	5329.8	62092.1	207684.0	11.7	39.0
5	5115.8	5115.8	59307.5	207684.0	11.6	40.6

Table 8: The FOM Comparison of Fission

Depletion Cycle	FOM				SUBSPACE Speedup	
	Analog		SUBSPACE		Fast	Thermal
	Fast	Thermal	Fast	Thermal		
No depletion	3066.1	3880.5	33229.4	207684.0	10.8	53.5
1	3066.1	5068.5	29578.0	207684.0	9.6	41.0
2	2794.2	4619.0	27381.6	207684.0	9.8	45.0
3	2614.7	4322.2	16814.3	207684.0	6.4	48.1
4	1918.7	5329.8	15523.0	207684.0	8.1	39.0
5	1841.7	5115.8	14826.9	207684.0	8.1	40.6